

Received: 2018.10.09
Accepted: 2019.01.16
Published: 2019.05.16

Primary Acute Angle-Closure Glaucoma: Three-Dimensional Reconstruction Imaging of Optic Nerve Head Structure in Based on Optical Coherence Tomography (OCT)

Authors' Contribution:
Study Design A
Data Collection B
Statistical Analysis C
Data Interpretation D
Manuscript Preparation E
Literature Search F
Funds Collection G

ABEF 1,2 **Yi Wang**
BD 2 **Di Chen**
EF 3 **Wen Yang**
C 4 **Qianqian Cui**
EF 3 **Weijie Hou**
DE 1,2 **Wenhui Han**
E 3 **Xiaohua Huang**
E 1 **Wen Lu**
E 5 **Zilong Yuan**
B 2 **Jiumin Yuan**
B 2 **Yufang Teng**
ABE 3 **Jianfeng Qiu**

1 Department of Ophthalmology, Taishan Medical University, Taian, Shandong, P.R. China
2 Department of Optometry, Taishan Medical University, Taian, Shandong, P.R. China
3 Department of Radiology, Taishan Medical University, Taian, Shandong, P.R. China
4 Beijing Youan Hospital, Capital Medical University, Beijing, P.R. China
5 Department of Radiology, Hubei Cancer Hospital, Wuhan, Hubei, P.R. China

Corresponding Authors: Jianfeng Qiu, e-mail: jfqiu100@gmail.com, Yi Wang, e-mail: 346048368@qq.com

Source of support: The authors thank the Shandong Province University Science and Technology Development Plan (No. J15LL05), Natural Science Foundation of Shandong; contract grant number: ZR2016HM73

Background: In glaucoma, the cup to plate ratio enlargement is a recognized pathological phenomenon. At present, the research on optic nerve in China and abroad mainly focuses on 2-dimensional research, and the measurement of 3-dimensional volume data is less well studied. Therefore, the recognition of 3-dimensional morphological changes is conducive to timely clinical intervention to prevent or slow down progressive vision loss.

Material/Methods: In this paper, optical coherence tomography (OCT) volume imaging technology was used to analyze and compare the morphological changes of primary acute angle-closure glaucoma in three-dimensional morphology, reconstruct the volume data of three-dimensional optic nerve head (ONH), and make morphological measurements.


Results: The rim width of the glaucoma group was significantly lower than that of the control group, and the average volume and intraocular pressure of the optic cup were significantly increased ($P < 0.05$), while the rim width and intraocular pressure of the other group were not significantly changed ($P > 0.05$).

Conclusions: We used three-dimensional reconstruction to identify OCT images between glaucoma patients and the control group with significant differences.

MeSH Keywords: **Glaucoma • Imaging, Three-Dimensional • Neural Tube**

Abbreviations: **IOP** – intraocular pressure; **3D** – three dimensional; **ONH** – optic nerve head; **OCT** – optical coherence tomography; **RNFL** – retinal nerve fiber layer; **N-NCO** – narrowest neural canal openings; **RPE/BM** – retinal pigment epithelium/Bruch's membranes; **C/D** – cup/disc ratio; **LC** – lamina cribrosa; **2D** – two dimensional; **CLAHE** – contrast limited adaptive histogram; **SNR** – signal to noise ratio; **CMPR** – cure MPR; **MPR** – multiplanar reconstruction; **FEM** – finite element method

Full-text PDF: <https://www.medscimonit.com/abstract/index/idArt/913541>

 2553

 1

 4

 32



Background

In 3-dimensional (3D) volume data, the nerve tissue in the optic nerve head (ONH) is shown and measured separately, and can be viewed internally by cutting at any angle without a block. After enhancement of the signal to noise ratio (SNR) and contrast, the nerve structure can then be defined to 4 significant figures. The improved 3D scan and reconstruction of the ONH provides more detail and clinical information. The 3D/2-dimensional (2D) parameters measured as 3D volumes of the ONH, provide supplemental information to evaluate glaucoma, in addition to the 2D fundus imaging technique.

In glaucoma patients, the ONH is the most vulnerable region of the posterior eye, owing to the mechanical weakness of this structure compared with the sclera [1,2]. Morphological differences can be observed between glaucoma and control eyes. While changes in several 1-dimensional and 2-dimensional (2D) parameters were well described, 3D morphological analysis can provide valuable additional information on complex structural distortions, including the deeper vertical nerve structures. Compared with control groups, the greatest differences in the 2D measurements the optic cup and rim has been reported in previous studies [3,4]. Thus, the upper surface of the ONH showed the greatest degree of structural deformation, and this was reflected by the 3D data. The nerve tissue in and around the ONH was markedly compressed. These 2D and 3D dimensions of the cup and rim may provide additional diagnostic criteria for glaucoma.

Glaucoma is the leading cause of age-related blindness [5–7]. It is characterized by progressive structural damage to the optic nerve and death of retinal ganglion cells [8], and is usually associated with chronically elevated intraocular pressure (IOP) [9]. High IOP causes structural deformation of the ONH [10–13], which may ultimately destroy nerve tissue. These morphological changes can be assessed using a variety of imaging modalities, including optical coherence tomography (OCT) [14,15]. Morphological changes to the ONH not only reflect disease onset and progression, but may also be useful as diagnostic markers [16–18]. Defining relevant morphological parameters for detection is critical because damage is irreversible, but it can be halted or slowed by IOP-lowering drugs [9].

Many studies have examined the morphological changes in the optic nerve and ONH in glaucoma patients. ONH morphology was often expressed by the ratio of optic cup to optic disc diameter (cup/disc ratio, C/D), which is increased in glaucoma [5,8,13]. Histological sections revealed obvious differences in ONH structure between glaucomatous and normal eyes [16,17]. Analyses of the neural canal opening (NCO) morphology also revealed structural changes during glaucoma [12]. Using finite element model analyses, they found that the ONH/

NCO morphology was affected by high IOP [18–20]. It has been reported that acute IOP elevation in monkeys altered lamina cribrosa shape, resulting in injury to the optic nerve. In recently years, some studies have used *in vivo* OCT to study the early morphological changes during glaucoma [21], and analyses of deep structures of the eye with 3D resolution close to that obtained by tissue histology [22,23]. Compared with 2D measurement results in the fundus, the 3D morphological data obtained from slice images have provided more accurate information, with nerve tissues not overlapping other tissues, and tissue slice images with minimum intervals. From 3D volume OCT images, additional morphometric parameters can be measured, such as the longitudinal C/D of the ONH [24,25] to identify more subtle changes associated with glaucoma [4], particularly in the acute stage.

Although there are some research studies about morphometric change of ONH using OCT image, the advantages of 3D imaging of ONH still have not been sufficiently studied to analyze the development of glaucoma. Some basic and clinic research still is performed based on the 2D fundus of ONH, measurement limited 3D dimensions of optic nerve tissues by the n-series tomography. The 3D ONH morphometric parameters, or some 2D parameters only determine volume data, which could be more efficiently extracted from the OCT volume data. Based on these shortages, we reconstructed and measured 3D morphometric changes of the ONH in acute angle-closure glaucoma and healthy samples. The dimensions of retinal nerve fiber layer (RNFL), optic cup, rim, NCO, narrowest neural canal opening (N-NCO), and retinal pigment epithelium/Bruch's membrane (RPE/BM) (3D and 2D) were extracted and measured in all samples as 3D series ONH volume data. As morphometric features, the parameters of 3D ONH may more accurately reflect the optic nerve tissue changes in 3D tissues and could supplement current methods to evaluate glaucoma by 2D fundus imaging.

Material and Methods

Patients

From December 2012 to August 2018, 16 eyes with primary acute angle-closure glaucoma and 21 normal individuals were selected for the study from the Department of Ophthalmology, Affiliated Hospital of Taishan Medical University. The samples selected in the study included 9 patients with acute angle-closure glaucoma. Inclusion criteria for the glaucoma group were definitive glaucoma diagnosis in the absence of diabetes mellitus or other optic nerve injuries and visual system traumas. The objective clinical diagnosis examinations of glaucoma were the comprehensive appearance of IOP (≥ 21 mmHg), C/D (enlarged cup) and abnormal visual field. At the time of initial

diagnosis of acute glaucoma, without any eye medical treatment and OCT imaging before, the whole ONH could be imaged by OCT volume scanning. The complete ONH volume data was obtained by 3D measurement. All 3D eye images showed cup bottoms without any image defects.

The IOP of glaucoma patient group IOP was ≥ 21 mmHg, with a C/D ≥ 0.6 . As the control group, the healthy eyes IOP between 15 mmHg and 20 mmHg, clinically normal C/D and visual field. All IOP data were obtained using a tonometer (TOPCON CT-80A; TOPCON, Tokyo, Japan). Each eye underwent basic fundus imaging by OCT using the Heidelberg SPECTRALIS®HRT+OCT, B-Scan module (Heidelberg Engineering, Heidelberg, Germany). This study was approved by the Ethics Committee of Taishan Medical University for research involving human participants, and adhered to the tenets of the Declaration of Helsinki.

Imaging and processing

All data were reviewed and confirmed by an ophthalmologist with experience in glaucoma diagnosis for at least 15 years (YT). For 3D volume imaging, every eye was scanned by longitudinal series tomography centered on the ONH with a $512 \times 512 \times 496$ 3D matrix in a $5.7 (5.8) \times 5.4 \times 6.2$ mm³ field of view (FOV). To eliminate the impact of OCT implanted software, we exported the raw image data to a desktop computer and performed the series processing separately.

Using a separate computer, the raw data (image stacks) were compiled into 3D volume data after preprocessing and rigid affine transformation. The preprocessing included a ratio transform, noise reduction, image enhancement, and slice interpolation, by using MATLAB software (MATLAB 6.0; The Math Works Inc., Natick, MA, USA). In each original image, the display ratio was transformed from 3: 2 to 3: 1, which had a uniform ratio conforming to the raw imaging field ($5.7 (5.8) \times 5.4 \times 6.2$) mm³ [24,26]. Then, we applied the median filter to control the image noise, to provide a good SNR image for clinicians. The contrast limited adaptive histogram (CLAHE) method was used for every image enhancement to strengthen the contrast of different layers of the retina and to limit the high contrast background. The algorithm was successfully used in fundus enhancement [15]. After filtering and CLAHE, the average SNR of the tomography slices increased to 36.88 from 9.77. The final preprocessed data are shown in Figure 1, and all preprocessing was supervised and validated by an ophthalmologist.

Measurements

Measurements and analyses of 3D morphology were all based on volume data, which was reconstructed by volume rendering and multilane reconstruction (MPR). Some verifications were

aided by cure MPR (CMPR). After interpolated volume rendering, the matrix of 3D ONH was $512 \times 512 \times 496$ mm³, and the voxel size was $0.01 \times 0.01 \times 0.1636$ mm³. Anatomical locations and reference points were identified by an experienced physician with 3D view MIMICS (MIMICS15.0; Materialize Inc., Leuven, Belgium) software. The ophthalmologist (DC) selected landmarks and drew color points on the 2D/3D images. A 3D view sample of the marker is shown in Figure 2. The manually selected method in 3D perspective was verified to be effective and successful [15,27]. The optic cup, optic rim, RNFL, N-NCO, and RPE/BM can be marked by using the method.

The areas and volumes of the nerve structures were calculated from the measured distances between points. The 2D information included the area of the rim, N-NCO, and the boundaries of the RPE/BM. The 3D measurements included the volume of the optic cup and rim. There were some parameters of N-NCO and RPE/BM defined as 3D data, including the inclination and round degree, since the measurement was performed on the 3D reconstructed ONH rather than on each signal slice. To avoid introducing auto-segmentation algorithm errors, all measurements and calculations were completed manually, and the data reported were averages of 3 separate measurements per subject. After the measurement, the marked positions of all optic nerve tissues were reviewed and confirmed by another physician.

The reference point locations from one typical OCT image in the central cross-section of the ONH are shown in Figure 3. For rim and cup markings, we used a reference plane 0.1500 mm above the RPE. According to Leung [25], measurements using this plane yielded better performance data for glaucoma analyses.

Statistical analyses

All statistical analyses were conducted using SPSS 22.0 software (SPSS Inc., Chicago, IL, USA). Levine's test was used to test whether variances from both of the groups were equal, and the SPSS software provided *t*-test values for equal variances assumed and Mann-Whitney U test values for unequal variances assumed. Furthermore, Spearman correlation was performed for the correlation between intraocular pressure and indexes with significant changes in glaucoma group. This is an exploratory research, so we didn't perform any correction. *P*<0.05 was regarded as statistically significant.

Results

This study included 37 eyes of which 16 eyes were from patients with primary acute angle-closure glaucoma and 21 normal eyes were from healthy individuals used as controls. There were 12 dimensions of optic nerve tissues in ONH detected

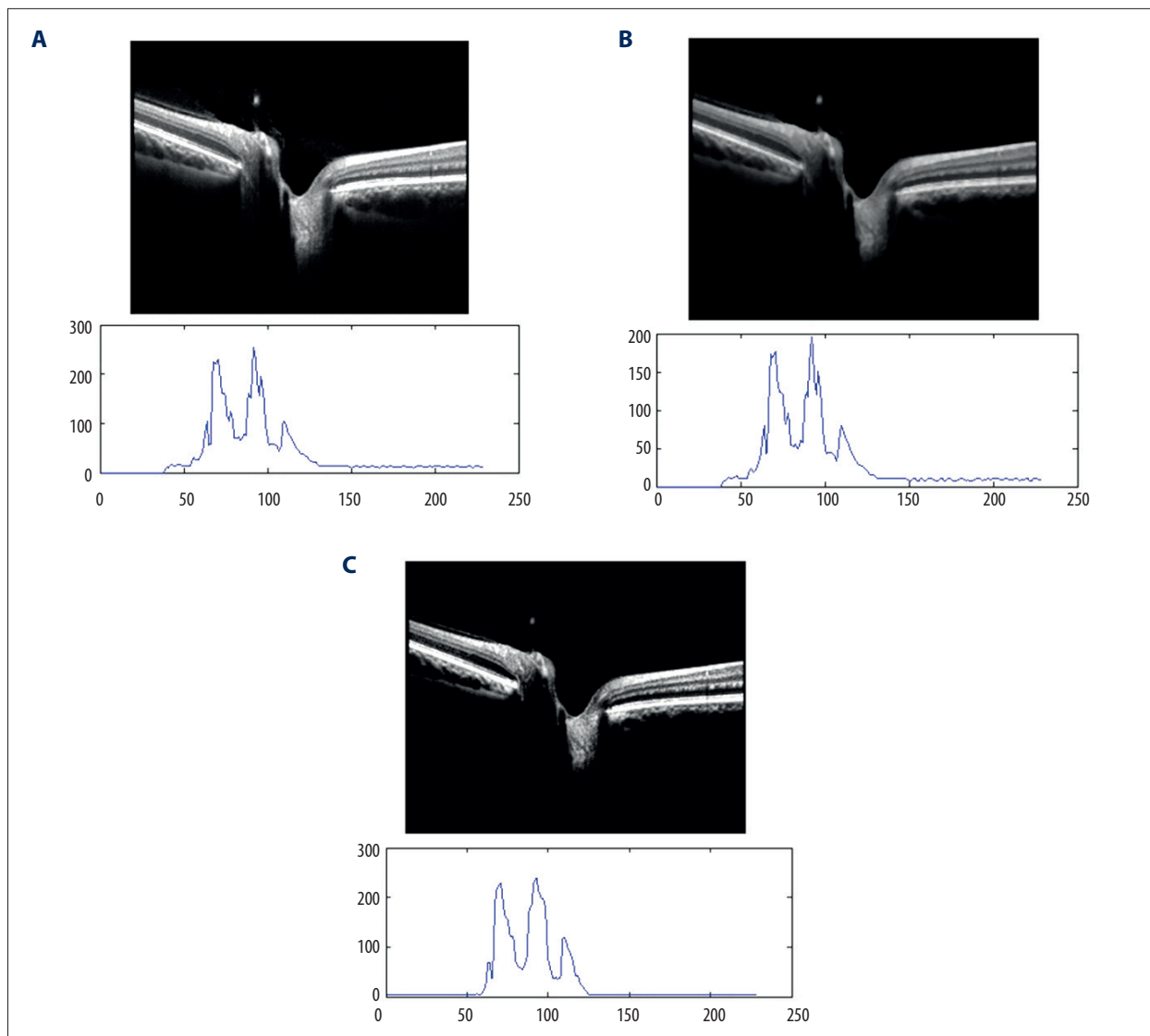


Figure 1. The processing of OCT images. **(A)** Raw image of the ONH. The bottom figure is the profile of the white line in the top OCT image. Obvious noise is shown. **(B)** The processed filtered image shows increased SNR, but the image still lacks contrast. **(C)** The processed image (by med-filter and CLAHE), with significantly improved contrast and gray level. The SNR was increased in the profile. OCT – optical coherence tomography; ONH – optic nerve head; SNR – signal to noise ratio; CLAHE – contrast limited adaptive histogram.

and compared, including RNFL thickness, the widths, and areas of the optic cup, rim, N-NCO and volumes of the optic cup and rim. The results are shown in Table 1. The relationship between the parameters of ONH and IOP. The results are shown in Figure 4.

There were 2 differences in all morphometric parameters studied between glaucoma and control groups. The 2 differences were noted in the optic cup volume ($Z=-2.545$, $P=0.01$) and rim width ($Z=2.974$, $P=0.003$), others no difference ($P>0.05$), with a particularly dramatic increase in optic cup volume in glaucoma patients. In the glaucoma group, the reduction of rim

width was obvious, and was thought to relate to optic nerve degeneration and ONH deformation. Moreover, the intraocular pressure of glaucoma is always greater than the intraocular pressure of normal eyes ($Z=-5.169$, $P<0.001$).

Analyze and compare the rim width, optic cup volume and intraocular pressure of glaucoma and normal eyes. It can be seen in Figure 4, the rim width was negatively correlated with the intraocular pressure value ($r=-0.579$, $P<0.001$) and the optic cup volume was positively correlated with intraocular pressure ($r=0.536$, $P<0.01$).

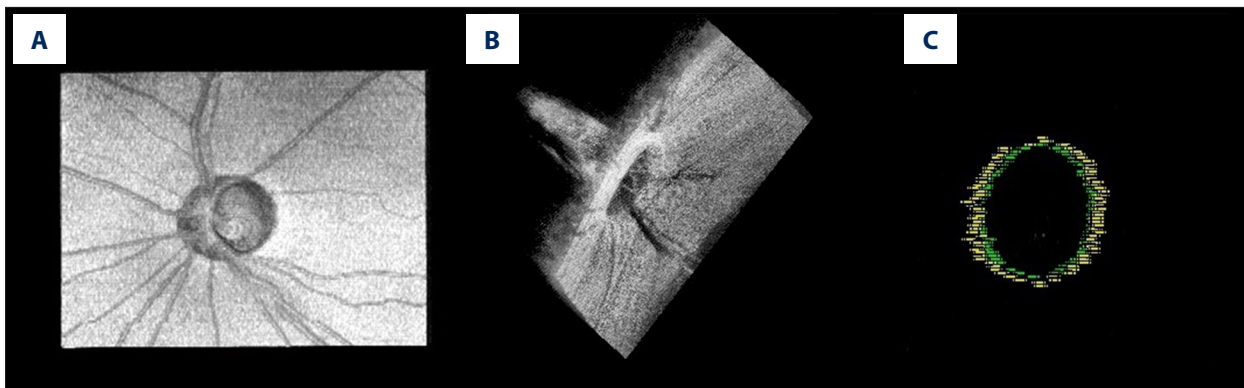


Figure 2. The 3D volume of the ONH and 3D view of the NCO marker. (A) Top view of the 3D volume of the ONH. (B) Side view of the ONH, with the 3D ONH clearly countered and complete in 3D form. Every measurement mark can be located in the real voxel of the ONH volume. (C) The 3D view of the NCO. The yellow color marks the RPE/BM and blue designates the narrowest NCO. 3D – 3-dimensional; ONH – optic nerve head; NCO – neural canal opening; RPE/BM, RPE – retinal pigment epithelium/Bruch's membrane.

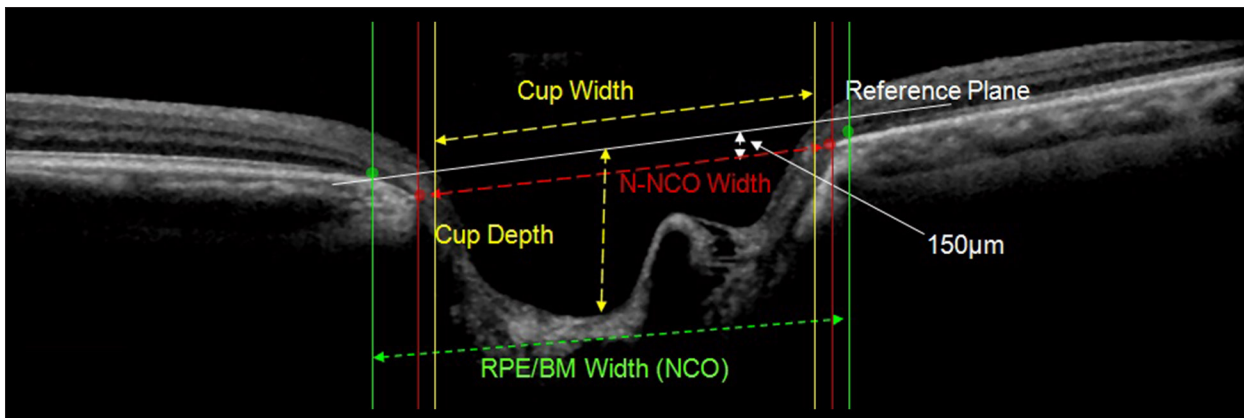


Figure 3. The reference points used to measure the morphology of the ONH. The width of the NCO is indicated by the green line joining the top and inner edges of the RPE. The reference plane was determined by tracing a line parallel to the NCO width plane with an offset of 0.1500 mm (white line). On this reference plane, the internal diameter of the rim edge was the cup diameter (width). The N-NCO was determined by the innermost and inward fold point of the choroid. ONH – optic nerve head; NCO – neural canal opening; N-NCO – narrowest neural canal opening; RPE – retinal pigment epithelium.

Discussion

We compared all morphometric dimensions of the ONH region between glaucoma patients and matched controls using 3D OCT volume imaging. Six parameters could only be tested by our 3D volume data, including the surface, and volume parameters. The data from the 3 areas were highly accurate because the results were averaged by data in different scan angles, which can only be obtained from volume data. These parameters were measured with micron resolution, and significant changes were observed in the rim width and optic cup volume of glaucoma patients.

The 3D analysis of the ONH using OCT, may reveal useful subtle morphological changes for early glaucoma diagnosis [28,29]. The optic nerve fibers within the ONH are directly affected by

the surface pressure load. As indicated in fundus images, rim area deformation caused thinning of the rim signal and cup expansion. The rim is composed of a large number of crowded optic nerve axons. Changes in rim area, height, and width are sensitive indicators of glaucoma. The change in volume due to deformation reflected complex morphological changes in the entire ONH but not simply tissue displacement. These complex 3D microscopic changes in the morphology of different ONH structures may provide additional insight into glaucoma pathogenesis.

In addition to the obvious deformation of the ONH, the rim width and optic cup volume also obviously differed between the control and glaucoma groups, others no difference. All measurements of rim width and optic cup volume areas were performed at the same time as other ONH measurements.

Table 1. Morphological changes in the optic nerve head in glaucoma.

Structure	Parameter	Control	Glaucoma	T [#] /Z ^{&}	P
RNFL	Surface (mm ²)	57.4272±25.8947	59.9508±13.4119	-0.276 ^{&}	0.783
	Width (mm)	1.0437±0.4803	1.0499±0.3610	-0.245 ^{&}	0.806
Optic cup	Depth (mm)	0.2725±0.2190	0.3398±0.1611	-1.034 [#]	0.308
	Volume (mm ³)	0.5233±0.7172	1.0453±1.0430	-2.545 ^{&}	0.011
Rim	Width (mm)	0.4308±0.1832	0.2322±0.2469	2.974 ^{&}	0.003
	Depth (mm)	0.2186±0.0656	0.2202±0.0760	-0.067 [#]	0.947
	Surface (mm ²)	2.5605±1.3491	2.1264±1.6256	-0.399 ^{&}	0.690
	Volume (mm ³)	0.1429±0.1137	0.1099±0.0882	-0.736 ^{&}	0.462
N-NCO	Width (mm)	1.4108±0.2835	1.3927±0.3112	-0.092 ^{&}	0.927
	Surface (mm ²)	2.7087±0.9975	3.1343±1.6175	-1.019 [#]	0.315
NCO	Width (mm)	1.6934±0.3009	1.6322±0.3493	0.571 [#]	0.572
	Surface (mm ²)	4.0098±1.4993	4.0619±1.9455	-0.092 [#]	0.927
IOP		16.7143±2.2393	28.8750±10.6074	-5.169 ^{&}	0.000

Analysis of variance; RNFL – retinal nerve fiber layer; N-NCO – narrowest neural canal opening; RPE/BM – retinal pigment epithelium/Bruch’s membrane; IOP – intraocular pressure; statistical method: [&] Mann-Whitney, [#] T-test. *r* – correlation coefficient; *P*<0.05 remarkable; IOP – intraocular pressure; • – glaucoma, ◦ – emmetropia; statistical method: spearman correlation.

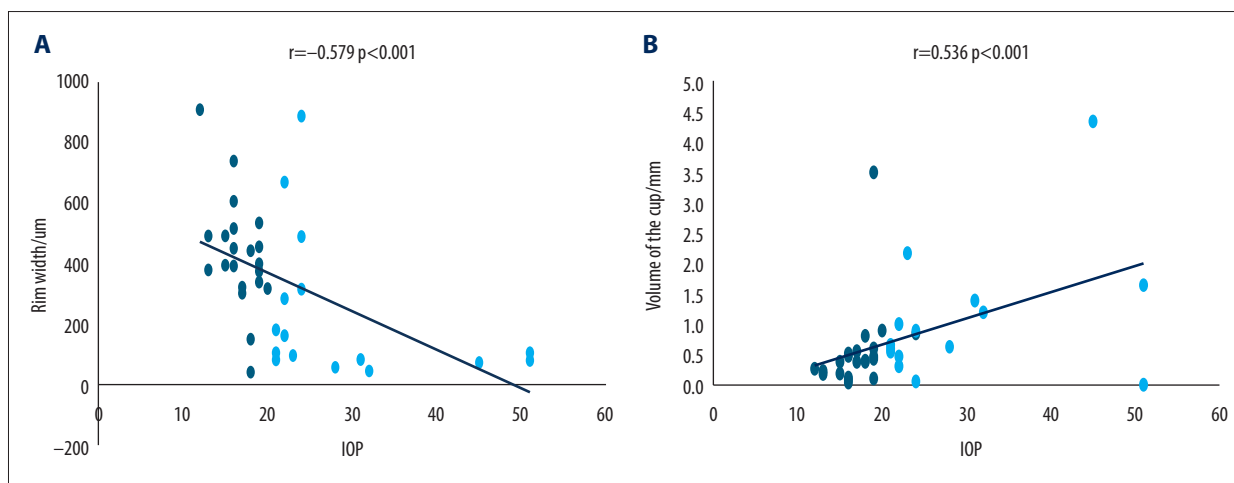


Figure 4. The relationship between the parameters of ONH and IOP. (A) Analysis of changes in intraocular pressure values between glaucoma and normal eyes with rim width. (B) Analysis of changes in intraocular pressure values between glaucoma and normal eyes optic cup volume. It can be seen that the rim width is negatively correlated with the intraocular pressure value ($r=-0.579, P<0.001$) and the optic cup volume is positively correlated with intraocular pressure ($r=0.536, P<0.01$). ONH – optic nerve head; IOP – intraocular pressure.

Several previous studies reported that the NCO (RPE/BM) was more stable than other ONH structures under elevated IOP [4,12,21,26,30]. In our study, there were statistically significant, albeit modest, differences between the rim width and optic cup volume groups. One possible reason could be insufficient sample size. Another confounding factor could be

that our cases of glaucoma were not grouped by severity of IOP elevation.

At present, studies of optic nerve connective tissue are the major focus of research into the pathogenesis of glaucoma [26]. In this study, the 3D morphology of the lamina cribrosa was

not measured. However, all data acquired for 3D reconstruction were retained for further structural analyses.

Three-dimensional volume information can also be used to explore the disc offset difference between the longitudinal image and the fundus image. However, disc measurements from fundus images may not detect the difference, and this could introduce subjective errors, especially in the measurement of C/D ratios [31,32]. If the measurements were made by using both fundus and tomographic OCT images, the subjective error caused by blood vessels and artifacts may be reduced and the C/D ratio may be determined more accurately.

The 3D volume analysis has another important application for biomechanical analyses in nerve structure finite element method (FEM) analysis. A model based on OCT images *in vivo* could be more complementary to FEM analysis than the section slice modeling procedure. The analytical results should become more accurate if the edge and depth structural image limitations can be solved in 3D imaging.

There were some limitations to this study. First, the OCT imaging should be improved. The edge of the lamina cribrosa and central blood vessels could not be captured in the image. Nerve structures were also not clearly shown in the OCT images. Second, the sample number was limited, therefore it was difficult to

compare these measurements to previous studies. For example, the rim area and N-NCO width were significantly different from reference samples [4,25]. However, the imaging did reveal differences in the N-NCO. Only larger ONHs allowed for imaging of the entire cup surface and RPE/BM termination with high quality. Therefore, the small ONHs included in our study could have contributed to group differences. Finally, we did not divide eyes according to IOP.

Conclusions

Three-dimensional OCT measurements demonstrated significant differences in the 3D morphology of the ONH in glaucoma patients. We suggest that glaucoma causes complex deformation of different ONH structures. In this study, we measured 12 separate morphometric dimensions in glaucoma and healthy eyes by 3D volume reconstruction of OCT images. The volume data and 3D measurement method may assist the understanding of deformation in spatial relationships. These deformations may provide additional markers for glaucoma diagnosis, and could facilitate a timelier diagnosis and treatment.

Conflicts of interests

None.

References:

1. Crawford Downs J, Roberts MD, Sigal IA: Glaucomatous cupping of the lamina cribrosa: A review of the evidence for active progressive remodeling as a mechanism. *Exp Eye Res*, 2011; 93: 133–40
2. Sigal IA, Ethier CR: Biomechanics of the optic nerve head. *Exp Eye Res*, 2009; 88: 799–807
3. Leung CK, Chan WM, Hui YL et al: Analysis of retinal nerve fiber layer and optic nerve head in glaucoma with different reference plane offsets, using optical coherence tomography. *Invest Ophthalmol Vis Sci*, 2005; 46: 891–99
4. Strouthidis NG, Fortune B, Yang H et al: Longitudinal change detected by spectral domain optical coherence tomography in the optic nerve head and peripapillary retina in experimental glaucoma. *Invest Ophthalmol Vis Sci*, 2011; 52: 1206–19
5. Quigley HA, Green WR: The histology of human glaucoma cupping and optic nerve damage: Clinic pathologic correlation in 21 eyes. *Ophthalmology*, 1979; 86: 1803–30
6. Weinreb RN, Aung T, Medeiros FA: The pathophysiology and treatment of glaucoma: A review. *JAMA*, 2014; 311: 1901–11
7. Tatham AJ, Weinreb RN, Medeiros FA: Strategies for improving early detection of glaucoma: The combined structure-function index. *Clin Ophthalmol*, 2014; 8: 611–21
8. Quigley HA, Addicks EM, Green WR, Maumenee AE: Optic nerve damage in human glaucoma. II. The site of injury and susceptibility to damage. *Arch Ophthalmol*, 1981; 99: 635–49
9. Bellezza AJ, Rintalan CJ, Thompson HW et al: Deformation of the lamina cribrosa and anterior scleral canal wall in early experimental glaucoma. *Invest Ophthalmol Vis Sci*, 2003; 44: 623–37
10. Wong TY, Hyman L: Population-based studies in ophthalmology. *Am J Ophthalmol*, 2008; 146: 656–63
11. Roberts MD, Liang Y, Sigal IA et al: Correlation between local stress and strain and lamina cribrosa connective tissue volume fraction in normal monkey eyes. *Invest Ophthalmol Vis Sci*, 2010; 51: 295–307
12. Xu L, Wang YX, Wang J, Jonas JJ: Mortality and ocular diseases: The Beijing Eye Study. *Ophthalmology*, 2009; 116: 732–38
13. Quigley HA, Nickells RW, Kerrigan LA et al: Retinal ganglion cell death in experimental glaucoma and after axotomy occurs by apoptosis. *Invest Ophthalmol Vis Sci*, 1995; 36: 774–86
14. Strouthidis NG, Yang H, Fortune B et al: Detection of optic nerve head neural canal opening within his tomorphometric and spectral domain optical coherence tomography data sets. *Invest Ophthalmol Vis Sci*, 2009; 50: 214–23
15. Qiu J, Qian X, Cui Q et al: Three-dimensional reconstruction and finite element modeling analysis of the rabbit optic nerve head in acute high intraocular pressure. *Japanese Journal of Applied Physics*, 2012; 51: 067001
16. Burgoyne CF, Downs JC, Bellezza AJ, Hart RT: Three-dimensional reconstruction of normal and early glaucoma monkey optic nerve head connective tissues. *Invest Ophthalmol Vis Sci*, 2004; 45: 4388–99
17. Downs JC, Roberts MD, Burgoyne CF, Hart RT: Multiscale finite element modeling of the lamina cribrosa microarchitecture in the eye. *Conf Proc IEEE Eng Med Biol Soc*, 2009; 2009: 4277–80
18. Sigal IA, Flanagan JG, Tertinegg I, Ethier CR: Reconstruction of human optic nerve heads for finite element modeling. *Technol Health Care*, 2005; 13: 313–29
19. Sigal IA, Flanagan JG, Ethier CR: Factors influencing optic nerve head biomechanics. *Invest Ophthalmol Vis Sci*, 2005; 46: 4189–99
20. Yang H, Downs JC, Sigal IA et al: Deformation of the normal monkey optic nerve head connective tissue after acute IOP elevation within 3-D histomorphometric reconstructions. *Invest Ophthalmol Vis Sci*, 2009; 50: 5785–99
21. Abramoff MD, Lee K, Niemeijer M et al: Automated segmentation of the cup and rim from spectral domain OCT of the optic nerve head. *Invest Ophthalmol Vis Sci*, 2009; 50: 5778–84
22. Inoue R, Hangai M, Kotera Y et al: Three-dimensional high-speed optical coherence tomography imaging of lamina cribrosa in glaucoma. *Ophthalmology*, 2009; 116: 214–22

23. Srinivasan VJ, Adler DC, Chen Y et al: Ultrahigh-speed optical coherence tomography for three-dimensional and en face imaging of the retina and optic nerve head. *Invest Ophthalmol Vis Sci*, 2008; 49: 5103–10
24. Hu Z, Abramoff MD, Kwon YH et al: Automated segmentation of neural canal opening and optic cup in 3D spectral optical coherence tomography volumes of the optic nerve head. *Invest Ophthalmol Vis Sci*, 2010; 51: 5708–17
25. Leung CK, Chan WM, Hui YL et al: Analysis of retinal nerve fiber layer and optic nerve head in glaucoma with different reference plane offsets, using optical coherence tomography. *Invest Ophthalmol Vis Sci*, 2005; 46: 891–99
26. Sibony P, Kupersmith MJ, Rohlf FJ: Shape analysis of the peripapillary RPE layer in papilledema and ischemic optic neuropathy. *Invest Ophthalmol Vis Sci*, 2011; 52: 7987–95
27. Qiu J, Qian X, Quan H et al: The *in vivo* 3D optic nerve head modeling based on human multimodality images. *World Congress on Medical Physics and Biomedical Engineering 2012 May 26–31, Beijing, China IFMBE Proceedings*, 2013; 39: 264–66
28. Sehi M, Iverson SM: Glaucoma diagnosis and monitoring using advanced imaging technologies. *US Ophthalmic Rev*, 2013; 6: 15–25
29. Roberti G, Centofanti M, Oddone F et al: Comparing optic nerve head analysis between confocal scanning laser ophthalmoscopy and spectral domain optical coherence tomography. *Curr Eye Res*, 2014; 39: 1026–32
30. Hu Z, Wu X, Hariri A, Sadda SR: Multiple layer segmentation and analysis in three-dimension spectral-domain optical coherence tomography volume scans. *J Biomed Opt*, 2013; (7): 76006
31. Drexler W, Fujimoto JG: State-of-the-art retinal optical coherence tomography. *Prog Retin Eye Res*, 2008; 27: 45–88
32. Schuman JS, Wollstein G, Farra T et al: Comparison of optic nerve head measurements obtained by optical coherence tomography and confocal scanning laser ophthalmoscopy. *Am J Ophthalmol*, 2003; 135: 504–12